# Gold Nanorod-Enhanced Fluorescence Enables Single-Molecule Electrochemistry of Methylene Blue

Weichun Zhang, Martín Caldarola, Biswajit Pradhan, and Michel Orrit*

*Huygens-Kamerlingh Onnes Laboratory, Leiden University, 2300 RA Leiden, Netherlands*

E-mail: orrit@physics.leidenuniv.nl

**Abstract**

Redox reactions are central to energy conversion and life metabolism. Here we present electrochemical measurements with fluorescent readout of the redox-sensitive dye Methylene Blue (MB), at the single-molecule (SM) level. To overcome the low fluorescence quantum yield of MB we enhanced fluorescence by individual gold nanorods to achieve the required sensitivity. By measuring *the same molecule* at different electrochemical potentials we determined the mid-point potential of each single molecule through its redox-induced fluorescence blinking dynamics.

## Keywords

Electrochemistry, Enhanced fluorescence, Gold nanorods, Methylene Blue, Single-molecule studies

Understanding electrochemical processes is important for a variety of fields such as electrocatalysis,[1,2] nanostructured material synthesis,[3,4] detection of ions[5] and biological processes,[6,7] among others. As redox reactions are extremely sensitive to the local environment, single-molecule (SM) techniques are naturally suited for such studies, since they provide local probes in the subnanometer range, with high sensitivity to changes of the physical and chemical properties of their local surroundings.[8] Electrochemistry with single-molecule sensitivity, proven for the first time by Fan and Bard,[9] was an important step towards understanding the environment's influence on electron transfer reactions. An alternative approach to the electrical output is the combination of electrochemical control and optical readout of the molecules involved in the reaction.[10] Such an approach has proved successful with single-molecule sensitivity thanks to surface enhanced Raman spectroscopy (SERS).[11–13] However, the behavior of molecules in the hot spots responsible for SERS signals is heavily influenced by interactions with the metal, in particular by possible hybridization of molecular orbitals with metal electronic states. Methods for the study of free molecules are thus needed. Alternatively, fluorescence spectroscopy was also used as a readout of the oxidation or reduction state, relying on the switching of a high quantum yield fluorophore between fluorescent and non-fluorescent states.[14] With this approach, however, SM electrochemical information cannot be accessed due to the fast diffusion of the molecules in solution. Here we worked with immobilized molecules to access millisecond time scales and took advantage of fluorescence enhancement provided by individual gold nanorods (AuNRs) to enable electrochemistry with fluorescence readout at single-molecule level, even for weak emitters. The enhancement factors in the near field of nanorods is much weaker than those in SERS hot spots, but they are felt at much larger distances, of the order of 10 nm, enabling the study of isolated molecules, free from interaction with the metal.

We studied the well-known redox-sensitive molecule Methylene Blue (MB), which is widely used for tissue staining[15,16] and for biochemical studies as a redox indicator.[17,18] MB is a brightly blue-colored, non-toxic, cationic thiazine dye.[19] MB undergoes the reversible

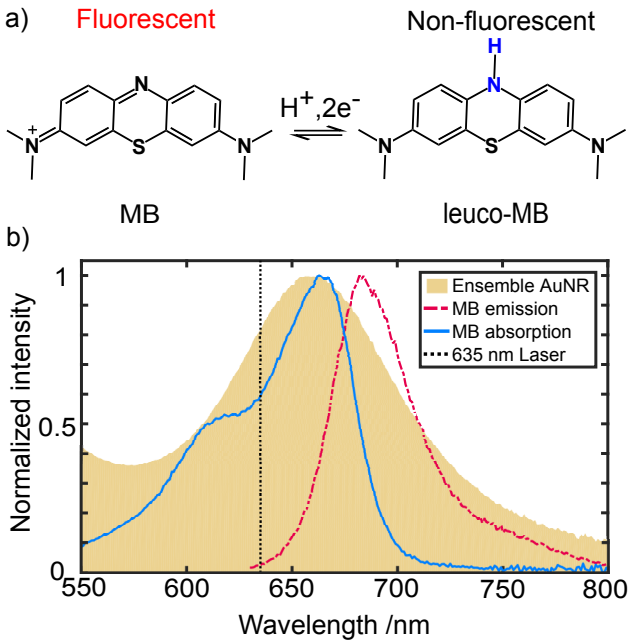


Figure 1: a) Two-electron reduction/oxidation reaction of Methylene Blue (MB). The reduced species, *leuco*-Methylene Blue is non-fluorescent under visible excitation. b) Absorption (blue) and emission (dashed red) spectra for MB in water. The shaded curve shows the UV-Vis extinction spectrum of a suspension of AuNRs in water. The vertical dotted line shows the wavelength used for fluorescence excitation of MB, on the blue wing of the longitudinal plasmon mode.

one-proton, two-electron transfer redox reaction shown in Figure 1a. The product of the reaction is colorless *leuco*-Methylene Blue, which does not absorb visible light.[20] Due to their low quantum yield[21] of $\sim 4\%$ it is difficult to detect single MB molecules by fluorescence. We performed a calibration experiment with MB molecules in solution to estimate the signal from an individual MB molecule and obtained 14 counts $s^{-1}$, which is well below our detection limit due to dark counts in the detector. Therefore, to achieve SM sensitivity, we propose to employ a fluorescence enhancement scheme.

For this purpose, we use AuNRs with an average size of 40 nm $\times$ 81 nm and a longitudinal surface plasmon resonance at about 660 nm. This plasmon resonance was selected to favor both excitation enhancement, *i.e.*, concentration of the excitation field at the laser wavelength (635 nm) at the tips of the AuNR, and emission enhancement, which depends on the overlap between the emission spectrum of the dye and the plasmon spectrum,[22,23] as

can be appreciated for the bulk spectra in Figure 1b. With these AuNRs we expect enhancement factors as high as $10^3$, which will allow detection of SM events above the fluorescence background from unenhanced molecules.

In order to perform electrochemical measurements with fluorescent readout, we used a confocal microscope previously described,[24] combined with the electrochemistry setup shown schematically in Figure 2a. The electrochemical cell presented three electrodes, consisting of a 30-nm thick gold layer deposited on the coverslip with a hole for optical access as the working electrode (WE), a saturated calomel electrode (SCE) as the reference electrode (RE), and a platinum wire as the counter electrode (CE). All the potentials throughout this work were reported relative to SCE. Isolated AuNRs and MB molecules were immobilized on the gold-free area of the coverslip. To allow reliable measurements of SMs, the MB layer had a concentration such that there was on average about 1 molecule in the electromagnetic near field of a AuNR. Because the MB molecules did not have direct electrical contact with the electrodes we used phenazine ethosulfate as an electron mediator to establish the redox potential of the medium surrounding the MB molecules. The working buffer was a pH=2 HCl-KCl buffer, in which the mid-point potential of phenazine ethosulfate matches that of MB so that the redox potential in the electrochemical cell can be controlled conveniently by the potentiostat. For further details about the experimental configuration and sample preparation, see the Supplementary Information.

Firstly, we used the electrochemistry-coupled fluorescence microscope to measure how the fluorescence of a small ensemble of $\sim 260$ unenhanced molecules immobilized on the glass surface responded to a static redox potential. We applied different potentials and recorded the corresponding fluorescence counts under 5 W/cm$^2$ illumination once the equilibrium was established. Figure 2b shows the intensity measured as a function of the applied voltage, where the switching of MB molecules from the dark to the bright state can be seen. We assign the hump at around $-50$ mV to molecule-substrate interactions, as it was not observed when doing the same measurement with MB solutions (data not shown). We modeled the

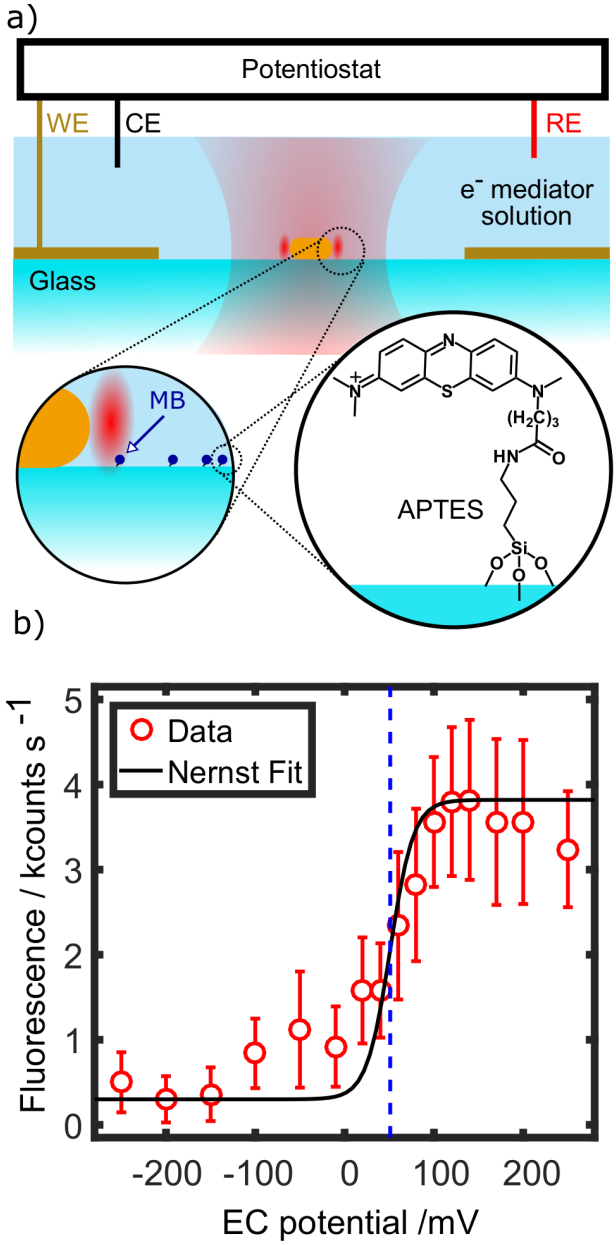


Figure 2: Electrochemistry with fluorescent readout. a) Scheme of the combined electrochemical-confocal setup and sample (WE: working electrode, CE: counterelectrode, RE: reference electrode). Individual AuNRs (not to scale) and MB molecules were immobilized on the glass surface. Phenazine ethosulfate mediates electron transfer between MB molecules and the gold film controlled via the potensiostat. b) Ensemble fluorescence response of $\sim$ 260 unenhanced MB molecules to the electrochemical potential, showing the controlled switching from the reduced state at low potentials to the oxidized state at high potentials. The black curve is a fit using the Nernst equation and the dashed line illustrates the obtained mid-point potential ($51 \pm 4$ mV).

ensemble of MB molecules with the Nernst equation (see the Supplementary Information) and obtained a mid-point potential of $51 \pm 4$ mV. This shows our capability of performing electrochemical experiments through fluorescence monitoring of a small ensemble.

Secondly, we turned to SM experiments, which are possible thanks to the enhancement provided by the AuNRs. We worked in the situation presented in Figure 2a, with one molecule in the near-field of the AuNR and several molecules in the confocal volume, contributing to the total signal. The low QY of MB has the advantage of providing a low background from those unenhanced molecules which does not obscure the signal from the enhanced molecule, *i.e.*, the signal from the enhanced molecule is high compared to the background. At SM level we expect to see fluorescence blinking induced by the dynamic equilibrium of the redox reaction. When the potential is set to the mid-point potential, we expect the molecule to spend half of the time reduced and half of the time oxidized, which will be evidenced by equal on- and off-times for the blinking. With the same reasoning, for reducing (oxidizing) potentials we expect that the molecule will spend more time in the off (on) state.

The fluorescence time trace of a single enhanced MB molecule is shown in Figure 3a, where SM reduction and oxidation events can be clearly distinguished, as well as a single-step bleaching event. The laser excitation peak intensity was 5 W/cm$^2$ . The bin time of 1 ms was chosen so that the on/off states can be clearly observed (for further discussion on this point, refer to the Supplementary Information). A step-detection algorithm[25] was used to extract the times associated to the switching events, shown in the figure in red. The obtained on- and off-times follow an exponential distribution with mean on- and off-times of $\bar{t}_{on} = 10.0 \pm 0.7$ ms and $\bar{t}_{off} = 39 \pm 2$ ms.

We further studied the blinking behavior of the *same* molecule at different electrochemical potentials. We detected the enhanced fluorescence from the same single molecules at different potentials successively under the same illumination conditions as before. Figure 4a shows three time traces (binned to 1 ms) obtained from such a molecule, where the blinking

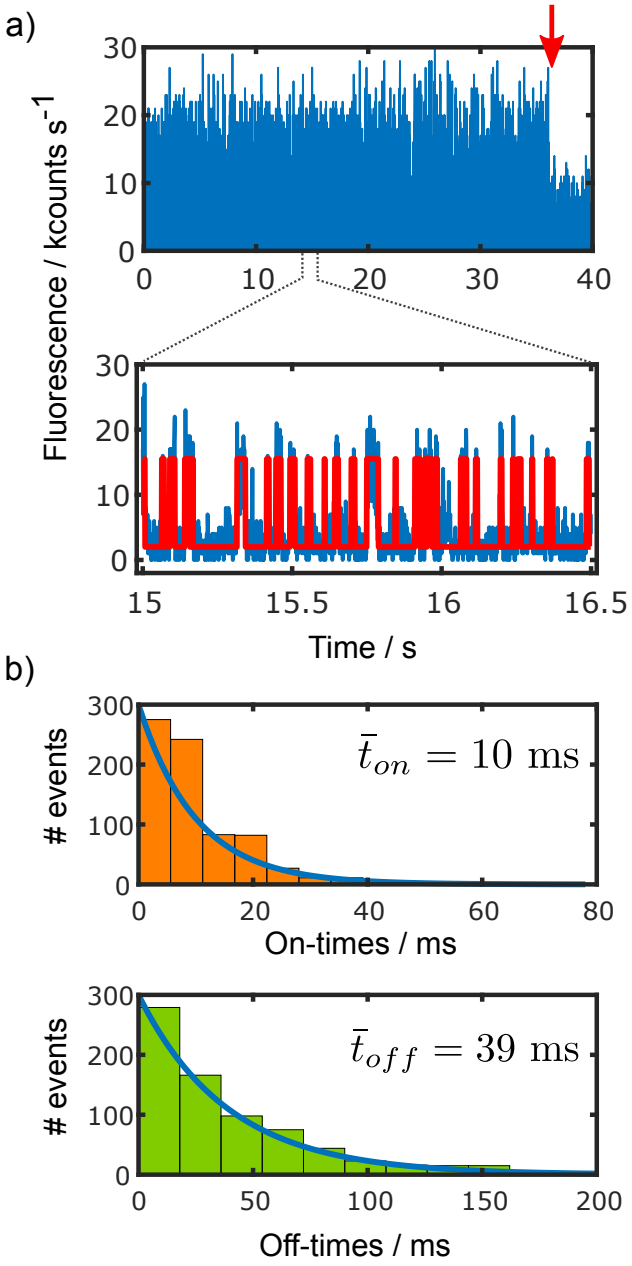


Figure 3: Single-molecule measurements at a fixed potential. a) (top) Fluorescent time trace from a AuNR-enhanced single molecule (binned to 1 ms) under an electrochemical potential of 80 mV. The arrow shows the one-step bleaching event. (bottom) Zoom that evidences the blinking behavior. The red trace was obtained through a step-detection algorithm. For this particular SM we estimated an enhancement factor value of $\sim 800$. b) Blinking events histograms for the on- (top) and off-times (bottom), showing an exponential distribution. The estimated mean times from single-exponential fits (blue solid lines) are shown on each plot.

dynamics is evidently responding to the electrochemical potential. The comparison of the traces shows that the on-time increases when the potential is increased while the off-time decreases, in accordance with the expected behavior. This general trend is observed in all the studied molecules.

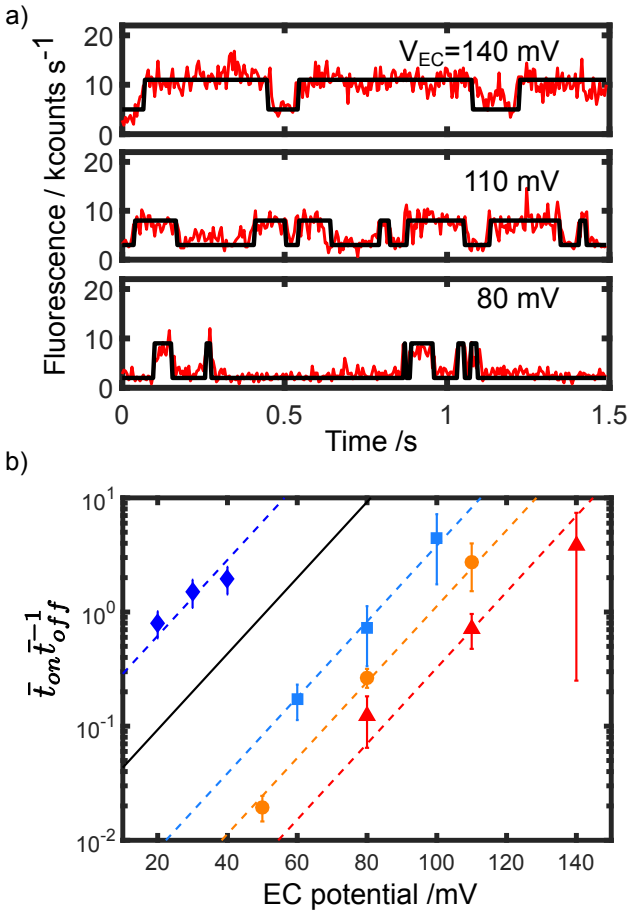


Figure 4: SM electrochemistry with fluorescence readout. a) Fluorescence time traces of the same single molecule at different potentials, where different blinking dynamics can be seen. b) The ratio $\bar{t}_{on}/\bar{t}_{off}$ is plotted as a function of the potential for some measured single molecules. Different symbols and colors represent different molecules. The red triangles correspond to the traces in a). The dashed lines are fits using the Nernst equation to extract the mid-point potential $E_0$ for each molecule, while the black solid line corresponds to the ensemble mid-point value extracted from data in Figure 2b.

To model the electrochemical switching of single molecules more quantitatively, we used the Nernst equation:

$$E = E_0 + \frac{k_B T}{ne} \ln\left(\frac{\bar{t}_{on}}{\bar{t}_{off}}\right), \tag{1}$$

where $E$ is the applied potential, $E_0$ the mid-point potential, $k_B$ the Boltzmann constant, $T$ the absolute ambient temperature, $n$ the number of electrons involved in the reaction, $e$ the electron charge and $\bar{t}_{on}$, $\bar{t}_{off}$ the mean on and off blinking times. Figure 4b shows several $\bar{t}_{on}/\bar{t}_{off}$ values (symbols) and fits with the Nernst equation to obtain $E_0$ (dotted lines). The measured distribution of mid-point potentials for single molecules can be modeled by a Gaussian with a central value of $\left\langle E_0^{SM} \right\rangle = 78.3 \pm 0.1$ mV and a dispersion of $\sigma^{SM} = 21.1 \pm 0.1$ mV (see Supplementary Figure S5).

The average SM mid-point potential is significantly higher than the ensemble value for the laser intensity used (51 mV, see Figure 2b). To address this discrepancy, we performed the same ensemble measurements as in Figure 2b with varying excitation intensities and observed a clear increase in mid-point potential with increasing intensity (see Figure S6). This presents a possible explanation for the mentioned shift in the average mid-point potential: a molecule in the vicinity of the AuNR is excited by an enhanced field that can be as high as 300-fold,[23] therefore the expected mid-point potential for such a molecule will be shifted to higher values by the strong irradiation. In order to further support this interpretation, we performed power dependence measurements on single molecules, shown in figure S7. We found that the same molecule shows higher mid-point potential when excited at higher intensity (see figure S7a), supporting further that laser irradiation has some influence on the redox reaction. A quantitative characterization and a mechanistic study of this photo-induced redox reaction require more experimental and theoretical work.

In conclusion, we have presented a scheme to study electrochemical properties of Methylene Blue at single-molecule level using fluorescence readout. Despite the low quantum yield of MB we were able to detect SM fluorescence blinking due to the high enhancement factors given by individual gold nanorods. Our single-molecule study of the *same* molecule at different redox potentials reveals that a single molecule's fluorescence emission responds to the ambient redox potential according to the Nernst equation, albeit the effective mid-point potential may be altered by the probing light. Our technique could be applied to measure the

local redox potential in chemical or biological systems by single molecules and opens up the possibility of single-molecule electrochemical studies of a broader set of weakly fluorescent molecules.

## Acknowledgement

We would like to acknowledge financial support from NWO, the Netherlands Organization for Scientific Research. WZ acknowledges a PhD grant from the China Scholarship Council. We thank Dr. Robert Pansu (ENS Cachan) for suggesting a redox study of methylene blue and Prof. Dr. Marc Koper for fruitful discussions.

## References

1. Mao, X.; Hatton, T. A. Recent advances in electrocatalytic reduction of carbon dioxide using metal-free catalysts. *Industrial & Engineering Chemistry Research* **2015**, *54*, 4033–4042.

2. Koper, M. T. Structure sensitivity and nanoscale effects in electrocatalysis. *Nanoscale* **2011**, *3*, 2054–2073.

3. Yu, Y.-Y.; Chang, S.-S.; Lee, C.-L.; Wang, C. C. Gold nanorods: electrochemical synthesis and optical properties. *The Journal of Physical Chemistry B* **1997**, *101*, 6661–6664.

4. Li, G.-R.; Xu, H.; Lu, X.-F.; Feng, J.-X.; Tong, Y.-X.; Su, C.-Y. Electrochemical synthesis of nanostructured materials for electrochemical energy conversion and storage. *Nanoscale* **2013**, *5*, 4056–4069.

5. Byers, C. P.; Hoener, B. S.; Chang, W.-S.; Link, S.; Landes, C. F. Single-Particle Plasmon Voltammetry (spPV) for Detecting Anion Adsorption. *Nano Letters* **2016**, acs.nanolett.5b04990.

6. Goldsmith, R. H.; Tabares, L. C.; Kostrz, D.; Dennison, C.; Aartsma, T. J.; Canters, G. W.; Moerner, W. Redox cycling and kinetic analysis of single molecules of solution-phase nitrite reductase. *Proceedings of the National Academy of Sciences* **2011**, *108*, 17269–17274.

7. Salverda, J. M.; Patil, A. V.; Mizzon, G.; Kuznetsova, S.; Zauner, G.; Akkilic, N.; Canters, G. W.; Davis, J. J.; Heering, H. A.; Aartsma, T. J. Fluorescent cyclic voltammetry of immobilized azurin: direct observation of thermodynamic and kinetic heterogeneity. *Angewandte Chemie International Edition* **2010**, *49*, 5776–5779.

8. Lemay, S. G.; Kang, S.; Mathwig, K.; Singh, P. S. Single-molecule electrochemistry: present status and outlook. *Accounts of chemical research* **2012**, *46*, 369–377.

9. Fan, F.-R. F.; Bard, A. J. Electrochemical Detection of Single Molecules. *Science* **1995**, *267*, 871–874.

10. Hill, C. M.; Clayton, D. A.; Pan, S. Combined optical and electrochemical methods for studying electrochemistry at the single molecule and single particle level: recent progress and perspectives. *Physical Chemistry Chemical Physics* **2013**, *15*, 20797–20807.

11. Cortés, E.; Etchegoin, P. G.; Le Ru, E. C.; Fainstein, A.; Vela, M. E.; Salvarezza, R. C. Monitoring the electrochemistry of single molecules by surface-enhanced Raman spectroscopy. *Journal of the American Chemical Society* **2010**, *132*, 18034–18037.

12. Cortés, E.; Etchegoin, P. G.; Le Ru, E. C.; Fainstein, A.; Vela, M. E.; Salvarezza, R. C. Strong correlation between molecular configurations and charge-transfer processes probed at the single-molecule level by surface-enhanced Raman scattering. *Journal of the American Chemical Society* **2013**, *135*, 2809–2815.

13. Zaleski, S.; Cardinal, M. F.; Klingsporn, J. M.; Van Duyne, R. P. Observing Single, Heterogeneous, One-Electron Transfer Reactions. *The Journal of Physical Chemistry C* **2015**, *119*, 28226–28234.

14. Lei, C.; Hu, D.; Ackerman, E. J. Single-molecule fluorescence spectroelectrochemistry of cresyl violet. *Chem. Commun.* **2008**, 5490–5492.

15. Canto, M. I. F.; Setrakian, S.; Petras, R. E.; Blades, E.; Chak, A.; Sivak, M. V. Methylene blue selectively stains intestinal metaplasia in Barrett's esophagus. *Gastrointestinal endoscopy* **1996**, *44*, 1–7.

16. Wainwright, M.; Crossley, K. Methylene Blue-a therapeutic dye for all seasons? *Journal of Chemotherapy* **2002**, *14*, 431–443.

17. Kerman, K.; Ozkan, D.; Kara, P.; Meric, B.; Gooding, J. J.; Ozsoz, M. Voltammetric determination of DNA hybridization using methylene blue and self-assembled alkanethiol monolayer on gold electrodes. *Analytica Chimica Acta* **2002**, *462*, 39–47.

18. Farjami, E.; Clima, L.; Gothelf, K. V.; Ferapontova, E. E. DNA interactions with a methylene blue redox indicator depend on the DNA length and are sequence specific. *Analyst* **2010**, *135*, 1443–1448.

19. Michaelis, L.; Granick, S. Metachromasy of basic dyestuffs. *Journal of the American Chemical Society* **1945**, *67*, 1212–1219.

20. de Tacconi, N. R.; Carmona, J.; Rajeshwar, K. Reversibility of photoelectrochromism at the TiO2/methylene blue interface. *Journal of the Electrochemical Society* **1997**, *144*, 2486–2490.

21. Olmsted, J. Calorimetric determinations of absolute fluorescence quantum yields. *The Journal of Physical Chemistry* **1979**, *83*, 2581–2584.

22. Punj, D.; de Torres, J.; Rigneault, H.; Wenger, J. Gold nanoparticles for enhanced single molecule fluorescence analysis at micromolar concentration. *Optics express* **2013**, *21*, 27338–27343.

23. Khatua, S.; Paulo, P. M.; Yuan, H.; Gupta, A.; Zijlstra, P.; Orrit, M. Resonant plasmonic enhancement of single-molecule fluorescence by individual gold nanorods. *ACS nano* **2014**, *8*, 4440–4449.

24. Pradhan, B.; Khatua, S.; Gupta, A.; Aartsma, T.; Canters, G.; Orrit, M. Gold-Nanorod-Enhanced Fluorescence Correlation Spectroscopy of Fluorophores with High Quantum Yield in Lipid Bilayers. *The Journal of Physical Chemistry C* **2016**, *120*, 25996–26003.

25. Shuang, B.; Cooper, D.; Taylor, J. N.; Kisley, L.; Chen, J.; Wang, W.; Li, C. B.; Komatsuzaki, T.; Landes, C. F. Fast step transition and state identification (STaSI) for discrete single-molecule data analysis. *The journal of physical chemistry letters* **2014**, *5*, 3157–3161.